

# An Asymptotically Stable Switched System Visual Controller for Eye in Hand Robots

Nicholas R. Gans and Seth A. Hutchinson

ngans@uiuc.edu, seth@uiuc.edu  
Dept. of Electrical and Computer Engineering  
The Beckman Institute for Advanced Science and Technology  
University of Illinois at Urbana-Champaign  
Urbana, IL USA

*Abstract*— Visual servoing methods are commonly classified as image based or position based, depending on whether image features or the robot pose is used in the feedback loop of the control law. Choosing one method over the other gives stability in the chosen state but surrenders all control over the other, which can lead to system failure if feature points are lost or the robot moves to the end of its reachable space. We present a hybrid switched system visual servo method that utilizes both image based and position based control laws. Through a switching scheme we present, this method will provide asymptotic stability in both the image and pose and prevent system failure.

## I. INTRODUCTION

Visual servo control allows for the closed loop control of a robot end-effector through the use of image data. It provides a high degree of accuracy using even simple camera systems and offers robustness in the face of signal error and uncertainty of system parameters. There are two approaches to visual servo control: Image-Based Visual Servoing (IBVS), and, Position-Based Visual Servoing (PBVS). In IBVS, an error signal is measured in the image, and is mapped directly to actuator commands. In PBVS systems, features are detected in an image, and used to generate a 3D model of the environment. An error is then computed in the Cartesian task space, and it is this error that is used by the control system. There are extensive resources detailing these methods [1], [2], [3], [4].

It is well known that both methods have specific strengths and shortcomings [5]. While many of these can be overcome by a proper set up of the task, some are fundamental to the control law and cannot be easily detected or overcome. Specifically, by zeroing the error in the image space, IBVS provides no control over the specific position or velocity of the camera and may perform unnecessary motions which can even lead to system failure. Likewise, PBVS surrenders control of the image features which may allow them to leave the image and cause the system to fail.

We have proposed a switched system approach to visual servoing, and experimentally verified its potential [6]. We will now provide a mathematical proof of stability under a state dependent switching rule. Section II contains a brief introduction to Hybrid Switched Systems, and Section III will discuss image based and position based visual servo-

ing, the two systems which comprise our switched system. Section IV then details our switched system control method and offers a proof of asymptotic stability. Finally, Section V will present some experimental and simulated results.

## II. HYBRID SWITCHED SYSTEM CONTROL

The theory of hybrid switched control systems, i.e., systems that comprise a number of continuous subsystems and a discrete system that switches between them, has received notable attention in the control theory community [7], [8], [9]. In general, a hybrid switched system can be represented by the differential equation

$$\dot{x} = f_{\sigma}(x) : \sigma \in \{1..n\} \quad (1)$$

where  $f_{\sigma}$  is a collection of  $n$  distinct functions. For our purposes, it is convenient to explicitly note that the switching behavior directly affects the choice of the control input  $u$

$$\dot{x} = f_{\sigma}(x, u_{\sigma}) : \sigma \in \{1..n\}. \quad (2)$$

A useful interpretation is to consider  $\sigma$  to be a discrete signal, switching among discrete values in  $1..n$ . The value  $\sigma$  at time  $t$  determines which function  $f(x, u_{\sigma})$  is used. The signal  $\sigma$  is typically classified as state-dependent or time-dependent, depending on whether switches are caused by the state of  $x$  or the time  $t$ , although overlap does exist between these classes. We explored state-dependent switching method contingent on the state of the image plane or camera pose.

The systems we present are each comprised of two visual servo controllers; each visual servo controller provides a velocity screw,  $\dot{r} = [T_x, T_y, T_z, \omega_x, \omega_y, \omega_z]^T$ , and a switching rule determines which is used as the actual control input at each control cycle.

The stability of a switched system is not insured by the stability of the individual controllers. Indeed, a collection of stable systems can become unstable when inappropriately switched. As an illustration, Figure 1 (from [9]) shows trajectories for two asymptotically stable subsystems in (a) and (b). A set of switches resulting in a stable system is shown in (c), while a series of switches resulting in an unstable system are shown in (d).

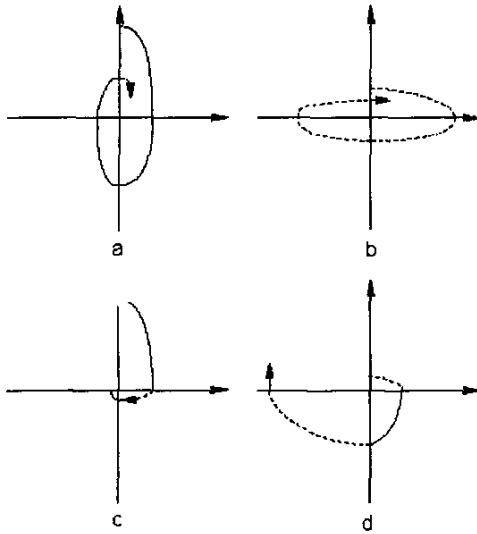


Fig. 1. trajectories of switched systems

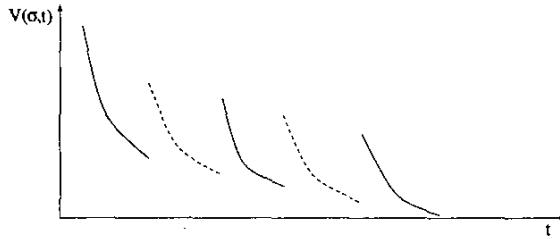


Fig. 2. stable family of Lyapunov function

Stability of a switched system can be extremely difficult to prove. Stability under arbitrary switching is often elusive. Generally this requires establishing a common Lyapunov function that works for all subsystems [9], [10]. Alternately, one can establish asymptotic stability under specific switching rule by establishing a family of Lyapunov functions for the systems such that at each switch, the value of their function at the end of that interval is less than the value of the function of the interval that proceeded it, as illustrated for a one dimensional family of two functions in Figure 2.2.

Given two linear subsystems,  $\dot{x} = A_1x$  and  $\dot{x} = A_2x$  a sufficient condition for the existence of a family of Lyapunov function is the existence of a stable convex combination  $A_c = \alpha A_1 + (1 - \alpha)A_2$ ;  $\alpha \in (0, 1)$ . Likewise, proof of stability for all convex combinations is sufficient to establish the existence of a common Lyapunov function and asymptotic stability under arbitrary switching. Identifying stable convex combinations known to be NP-hard [11]. Thus it is often necessary to establish proof of stability through less direct methods by proving boundedness of the system by appropriate switching.

### III. VISUAL SERVOING

Visual servoing is the use of image data in closed loop control of a robot. There generally considered to be two basic methods of Visual servoing, Image Based Visual Servoing (IBVS) and Position Based visual Servoing (PBVS). There exists a large body of work regarding these techniques. [1], [2], [3], [4].

The task in PBVS is to regulate the error between the current camera pose and the goal pose. Given a current camera position  $X$  and goal position  $X^*$  (from here on, variables in the goal configuration will be denoted with  $*$ ), the transformation relating them is described by a translation and rotation of the camera frame. The translation and rotation are quantified by  ${}^cT_c \in \mathbb{R}^3$  and  ${}^cR_c \in SO(3)$ , respectively. There are a number of ways to decompose the rotation matrix, we will use  $R \equiv [\omega_x, \omega_y, \omega_z]^T$ , which gives a measure of rotation about each 3D axis, and  $R \equiv u\theta$ , where  $\theta$  is a measure of rotation about the vector  $u$ .

With  $X$  and  $X^*$ , we define the pose error as

$$e_p = [{}^cT_c, u\theta]^T. \quad (3)$$

Given a collection of feature points in the image, there are numerous methods to extract the rotation and translation [12], [13], [14]. These methods differ in speed, accuracy and the number of feature points required. Some require a CAD model of the 3D points as well

The time derivative of  $e_p$  can be defined as

$$\dot{e}_p = L_p \dot{r}, \quad L_p = \begin{bmatrix} {}^oR_c & 0 \\ 0 & L_\omega {}^oR_c \end{bmatrix}$$

where  ${}^oR_c$  is the rotation matrix relating the orientation of the camera frame with the world frame. By choosing the goal pose to be the origin of our system, we get  $L_\omega = I_3$  and the system reduce to

$$\dot{e}_p = L_p \dot{r}, \quad L_p = \begin{bmatrix} {}^cR_c & 0 \\ 0 & {}^cR_c \end{bmatrix} \quad (4)$$

We can solve for  ${}^cT_c$  and  ${}^cR_c = u\theta$  using the computationally methods listed above and move the camera as follows

$$\dot{r} = -\lambda_p L_p^{-1} e_p = \begin{bmatrix} {}^cR_c & 0 \\ 0 & -L_\omega {}^cR_c \end{bmatrix} \begin{bmatrix} {}^cT_c \\ u\theta \end{bmatrix} \quad (5)$$

giving the proportional control law

$$\begin{aligned} \dot{e}_p &= -\lambda_p L_p L_p^{-1} \begin{bmatrix} {}^cT_c \\ u\theta \end{bmatrix} \\ &= -\lambda_p e_p. \end{aligned} \quad (6) \quad (7)$$

The matrix  ${}^cR_c$  is an element of  $SO(3)$  and thus has a determinant of one and  $L_p$  is always invertible.

Clearly, the error will tend to zero with time, thus the system is Globally Asymptotically Stable (GAS). While the position error tends monotonically to zero, but we have

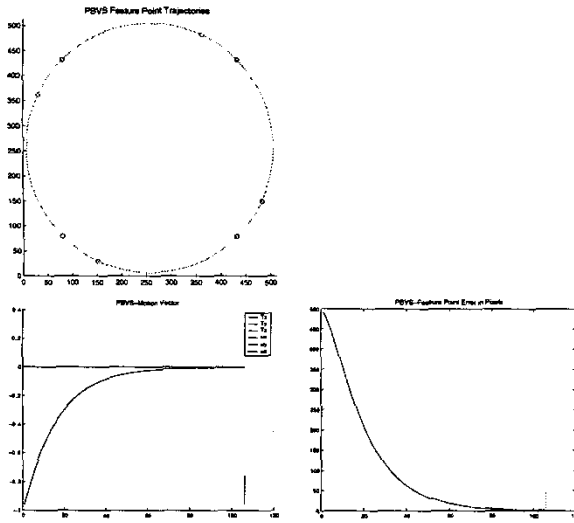


Fig. 3. Example Of Typical Motions For Feature Points And Camera In PBVS

no control over the position of the image points. If there is any rotation present the feature points will move along curves as the camera undergoes rotation and translation, this is seen in Figure 3. In a physical system we have a limited imaging surface and it is possible for the feature points to leave the image. In this case the system can no longer reconstruct the motion parameters and we cannot complete the task. We will define failure of a visual servo system to be any situation in which it does not successfully zero the error.

In Image Based Visual Servoing, the task we are regulating exists in the image space. Given collection of  $n$  image point,  $\mathbf{p}_j$ ,  $j \in \{1 \dots n\}$ , we can define the error between a point  $\mathbf{p}_j$  and its position in a goal image

$$\mathbf{e}_{ij} = \mathbf{x}_j^* - \mathbf{x}_j. \quad (8)$$

The motion of an image point is related to the motion of the camera by

$$\dot{\mathbf{x}} = \mathbf{L}_i \dot{\mathbf{r}} \quad (9)$$

$$= \begin{bmatrix} \frac{1}{z} & 0 & -\frac{x}{z} & -xy & 1+x^2 & -y \\ 0 & \frac{1}{z} & -\frac{y}{z} & -1-y^2 & xy & x \end{bmatrix} \begin{bmatrix} T_x \\ T_y \\ T_z \\ \omega_x \\ \omega_y \\ \omega_z \end{bmatrix}$$

where  $\mathbf{L}_i$  is the image Jacobian[1], [2].

We can take the time derivative of (8) and combine it with (9) to get

$$\dot{\mathbf{e}}_{ij} = \mathbf{L}_i \dot{\mathbf{r}}. \quad (10)$$

If we have three or more feature points, we can stack the vectors and matrix of equation (10) to build a full rank Image Jacobian, and solve for the robot motion as

$$\dot{\mathbf{r}} = \lambda_i \mathbf{L}_i^+ \mathbf{e}_i. \quad (11)$$

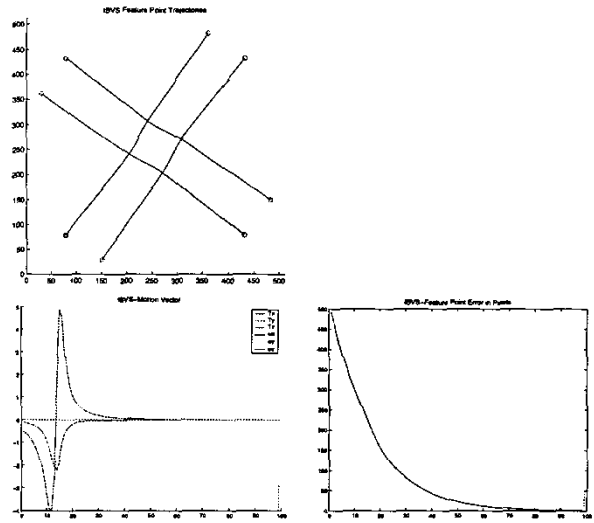


Fig. 4. Example Of Camera Retreat Under IBVS With Large Rotation

This gives the proportional control law

$$\begin{aligned} \dot{\mathbf{e}}_i &= -\lambda_i \mathbf{L}_i \mathbf{L}_i^+ \mathbf{e}_i \\ &= -\lambda_i \mathbf{e}_i \end{aligned} \quad (12)$$

This system is clearly Asymptotically Stable (AS). It would appear to be GAS, but there are known to be singularities that can arise in the image Jacobian; there also can exist local minima since the ambiguity of depth during projection means it is possible that more than one pose may give rise to the same image Jacobian.

The singularities and local minima generally occur only with very specific feature point configuration and specific camera motions and are generally regarded as a class of non-general configurations. These configurations would also likely prevent the PBVS system from correctly computing the pose, but since they manifest themselves directly in the control law here, we limit the claim of IBVS to be Locally Asymptotically Stable (LAS). The region of convergence is very difficult to obtain, but the non-general configurations constitute a region of measure zero.

More troubling than the potential singularities or local minima is the phenomenon of camera retreat. Since the image trajectories will follow a straight line to their goal configuration, a change of scale must take place to turn the normally elliptical trajectories into straight lines. This scaling is achieved by pulling the camera back along its z-axis. An illustration of this phenomenon is given in Figure 4.

Corke and Hutchinson quantified this scaling as  $\frac{d_{target}}{d_{max}} = \cos \frac{\alpha}{2}$  [15]. This analysis is illustrated in Figure 5, where  $d_{target}$  is the depth to the feature point at the goal configuration,  $d_{max}$  is the maximum depth caused by camera retreat, and  $\alpha$  is the angle in the image plane between lines from the point's goal position and current position to the image center. Note that during zero rotation the ratio is one, while an angle of pi will cause an infinite retreat.

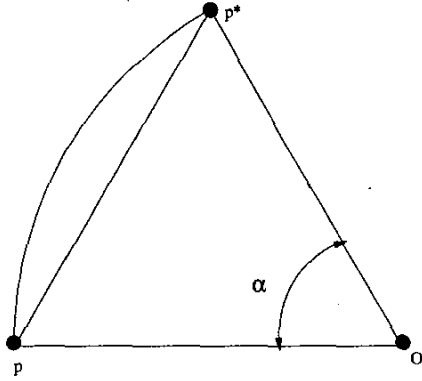


Fig. 5. Camera retreat model

Obviously a physical robot cannot perform an infinite camera retreat, most robot systems have a reachable space on the order of meters. Thus it is possible for the robot to extend to its joint limits during visual servoing, resulting in failure. Another scenario is that pull back can seriously affect the camera, causing the focus to be incorrect and adversely affecting the system, possibly resulting in failure.

#### IV. THE SWITCHED SYSTEM AND PROOF OF STABILITY

Since the strengths of PBVS compliment the weakness of IBVS and vice versa, it seems natural to design a system that switches between them to capture these strengths and minimize the weaknesses. Through this we hope to attain an asymptotically stable system. Furthermore, we seek to keep the system from ever failing due to lost feature points or the robot moving to the end of its reachable space. To achieve this we devised a switching rule that prevents failure, and prove that a finite number of switches must take place before we reach a position where both the position error and image error both decrease under either one of the visual servo systems.

Our method is basically to switch whenever the current system is in danger of failing. We define a threshold region for each system. For PBVS, this threshold will be a region in the image plane containing the image center that smaller than the image. The simplest region is defined by a circle of radius  $\varepsilon_p$  from the image center. For IBVS, the threshold will be a region within the robot configuration space that contains the object (by object we mean the rigid configuration of 3D points used for feature points). The simplest such region is a portion of sphere of radius  $\varepsilon_i$  and centered at a point on the object.

We also define two switching metrics. Define  $maxf$  as the greatest Euclidean distance in  $\mathbb{R}^2$  of each feature point to the image center. Define  $d_o$  as the distance from the camera to the object. If  $\frac{maxf}{\varepsilon_p}$  is greater than  $\frac{d_o}{\varepsilon_i}$  then begin servoing with IBVS in order to reduce the feature point error and in turn prevent  $maxf$  from becoming higher than it's final value. If  $\frac{d_o}{\varepsilon_i}$  is greater, then we begin with PBVS.

If the system we choose initially reduce has a ratio greater than one, reset the threshold to be equal to the current value of  $maxf$  or  $d_o$  as appropriate.

The system currently in use may see its switching metric rise. Whenever a metric reaches its threshold, switch to the other system. Neither system can fail, and furthermore there will be a finite number of switches before we converge to zero.

We make the following assumptions:

ASSUMPTION 1: The image features are well posed so as to rule out the existence of a local minimum.

ASSUMPTION 2: The feature points are static with respect to the world frame.

ASSUMPTION 3: One system, PBVS or IBVS, starts below its threshold.

ASSUMPTION 4: The goal image and pose are within the thresholds for both IBVS and PBVS.

The following Lemmas are stated without proof. Proofs are given in Appendix A

**Lemma 1:** The pose error  $e_p = 0$  if and only if the image error  $e_i = 0$

**Lemma 2a:** During PBVS the pose error  $e_p$  decreases monotonically while the image error  $e_i$  may increase or decrease

**Lemma 2b:** During IBVS the image error  $e_i$  decreases monotonically while the pose error  $e_p$  may increase or decrease

**Lemma 3:** For both IBVS and PBVS, there exists a range of camera positions where, under visual servo control, both the pose error  $e_p$  and image error  $e_i$  decrease to 0 as time goes to infinity. Additionally, if the difference between the goal and current pose consists of translation with a sufficiently small rotation, then we are within this region.

**Lemma 4:** During IBVS, the rotation component of the position error will be strictly non-increasing.

**Theorem:** Asymptotic stability can be achieved by switching between IBVS and PBVS systems. Furthermore, the switched system can zero the error in situations when IBVS, PBVS, or both would fail due to lost feature points or robot pose constraints.

**PROOF.** If the initial position is related to the goal position by a translation and sufficiently small rotation, then the system will be in the region where both errors decrease monotonically, as per Lemma 3. Since the goal configuration lies within both original threshold regions, and both errors are moving towards 0 monotonically, we have convergence to the goal position and neither of the metrics can reach their threshold level.

If the system is not in the region described by Lemma 3, the system we choose will monotonically decrease its error and the other system will increase its error. The decrease-

ing error will see its switching metric converge towards the goal value. The increasing error may be accompanied in an increase in the switching metric chosen for the current system. If the camera moves into the set of poses defined by Lemma 3, then again both errors will converge to 0 and we will have convergence.

If the system does not enter the region described in Lemma 3, the increasing error will eventually force the switching metric to reach its threshold. We then switch to the other visual servo system. The metric at its threshold must go down as its corresponding error will be decreasing towards zero. The error which was previously decreasing will begin increasing with a likely increase in its switching metric. At this point the system can enter the region described in Lemma 3 and converge to the origin or the increasing metric can increase to its threshold, in which case we switch again.

Repeating this process gives two possible results. The systems may eventually stop switching and converge to the origin and the switching metrics converge to their goal values, or the system can switch often and the metrics will converge towards their thresholds and the errors converge to some non-zero point. However, in the worst case scenario of rapid switching, neither system can increase its metric beyond its threshold so neither can fail. Moreover, PBVS will always reduce the rotational portion of the pose error, and by Lemma 4, IBVS will never increase the rotational pose error and may reduce it. Therefore, even in the case of rapid repeated switching, there can only be a finite number of switches before the majority of rotation will be completed and the current pose will lie in the region described by Lemma 3 and the error will converge to zero.  $\square$

We have thus proven the stability of our system under a specific switching rule. To achieve a stronger result, we must prove stability under arbitrary switching. This is a difficult problem for all but the simplest hybrid switched systems, and we have not finalized a proof at this time. However, the structure of our switched system lends hope that we can achieve this goal in the near future. We thus present partial results of our attempt to prove stability under arbitrary switching, and the avenues of our future investigation.

Firstly, since the error exists in two different spaces, we must build a common state space by combining them. This is accomplished mathematically by concatenating the state vectors and building appropriate plant matrices as seen in Equations (13) and (14), where we consider on the simpler situation of three feature points used for IBVS, providing a  $6 \times 6$  image Jacobian.

$$\begin{bmatrix} \dot{\mathbf{e}}_p \\ \dot{\mathbf{e}}_i \end{bmatrix} = \lambda_\sigma \mathbf{A}_\sigma \begin{bmatrix} \mathbf{e}_p \\ \mathbf{e}_i \end{bmatrix}, \quad \sigma \in \mathbf{P}, i \quad (13)$$

$$\mathbf{A}_p = - \begin{bmatrix} \mathbf{I}_6 & \mathbf{0} \\ \mathbf{L}_i \mathbf{L}_p^{-1} & \mathbf{0} \end{bmatrix}, \quad \mathbf{A}_i = - \begin{bmatrix} \mathbf{0} & \mathbf{L}_p \mathbf{L}_i^+ \\ \mathbf{0} & \mathbf{I}_6 \end{bmatrix} \quad (14)$$

We can investigate the stability of convex combinations of the form

$$\begin{aligned} \mathbf{A}_c &= \alpha \mathbf{A}_p + (1 - \alpha) \mathbf{A}_i; \quad \alpha \in (0, 1) \\ &= \begin{bmatrix} -\alpha \mathbf{I}_6 & -(1 - \alpha) \mathbf{L}_p \mathbf{L}_i^+ \\ -\alpha \mathbf{L}_i \mathbf{L}_p^{-1} & -(1 - \alpha) \mathbf{I}_6 \end{bmatrix} \quad (15) \end{aligned}$$

Asymptotic stability of a system described by  $\mathbf{A}_c$  could be proved if the real parts of all its eigenvalues are negative (a matrix that meets this criteria is said to be *Hurwitz*). However, the upper corner of the matrix is the inverse of the lower corner, which creates a linear dependence. This system will always have six negative eigenvalues and six eigenvalues equal to zero. In a linear time invariant system, the presence of zero eigenvalues would not rule out the possibility of stability, but hybrid systems require the stronger condition of asymptotic stability of the convex combination. Thus these results are inconclusive. They do not prove the existence of a Lyapunov function, but since no eigenvalue is positive, they do not rule out the existence either.

Further complicating the exploration is the fact that, the  $\mathbf{L}_p$  and  $\mathbf{L}_i$  matrices are typically time varying (due to concerns regarding time of computation, early experiments in visual servoing often kept the Jacobians constant, but this practice is no longer common). This requires us then to seek a solution  $\mathbf{P}(t)$  to the equation

$$\mathbf{A}_c^T(t) \mathbf{P}(t) + \mathbf{P}(t) \mathbf{A}_c(t) + \dot{\mathbf{P}}(t) \leq -\mathbf{Q}(t) \quad (16)$$

where  $\mathbf{P}(t)$  and  $\mathbf{Q}(t)$  are continuous, bounded and positive definite for all time and  $\mathbf{P}(t)$  is symmetric. Finding such a solution is quite difficult; in our preliminary investigations the existence of a solution  $\mathbf{P}(t)$  appears to be dependent upon the structure and condition of the image Jacobian, which in turn may be dependent on the camera motion and the properties of the feature being used. To our knowledge, an in depth investigation into the properties of the image Jacobian has not been performed.

## V. RESULTS

We have tested the switched system extensively in simulations and experiments. These results have appeared previously in [6]; we reproduce a select few to demonstrate the performance of our system under the described switching law.

### A. Simulations

We simulated the system with a typical camera, but allowed for ideal camera performance, robot performance, and depth estimation. We begin with a situation in which either PBVS or IBVS will likely fail to zero the error, a rotation of  $160^\circ$  about the optical axis with the feature points far from the image center. For all simulations, trajectories with black lines are motions performed by IBVS, while cyan lines are performed by PBVS.

The results of PBVS are seen in Figure 6. The first graph shows the feature point trajectories. The feature start too

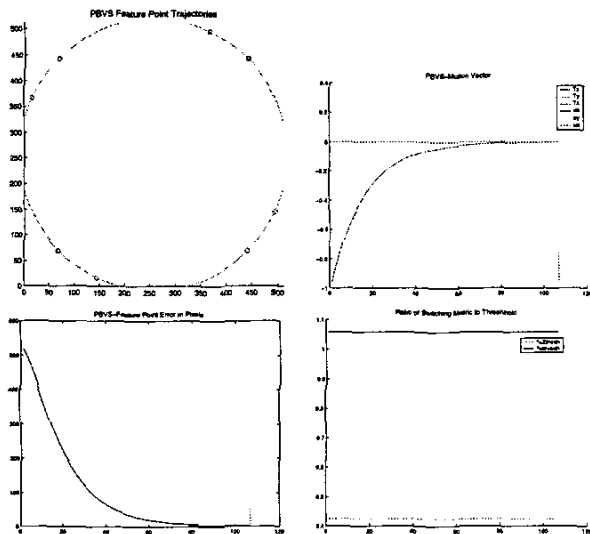


Fig. 6. PBVS Losing Feature Points

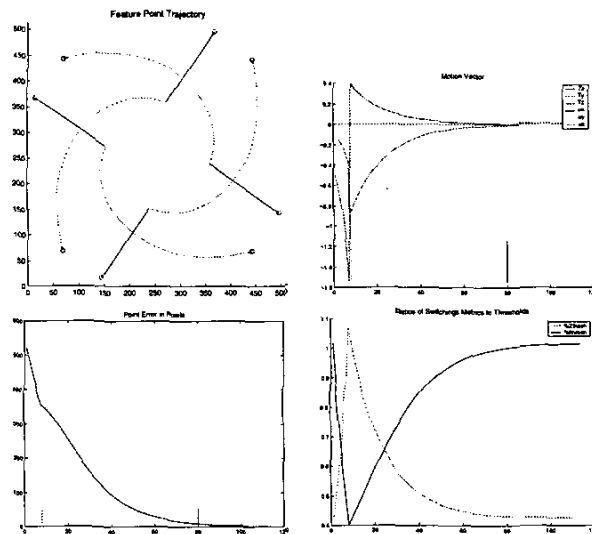


Fig. 8. Hybrid switched system successfully zeroing the error

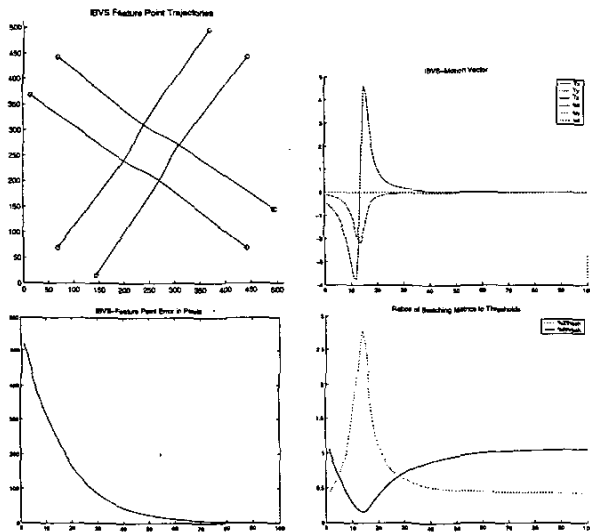


Fig. 7. IBVS Experiencing Severe Camera Retreat

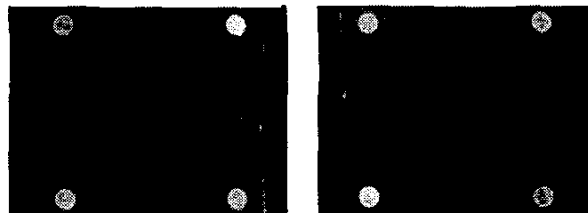


Fig. 9. Initial And Goal Images

close to the edge of the image, thus while the camera trajectory is smooth, feature points are lost.

The results of IBVS under the same motion are seen in Figure 7. The feature point trajectories are well behaved, but the camera retreat is very extreme. In this case it would retreat almost three meters, likely out of the reachable space of many robots.

Finally we see the results of the switched system in Figure 8. The feature points are near the edge of the image, so we use IBVS to pull the feature points towards their goals. When the camera retreat becomes too extreme we switch again to PBVS.

### B. Experimental Results

We now present experimental results. We used a Puma 560 robot arm and a Sony DFW-V500 color camera. The feature points are colored dots that allowed us to find the center points using each color channel. The pose difference between initial and goal is a large rotation about the optical axis, and the camera is physically near the feature points so they appear close to the edge of the image. This is arguably one of the most difficult visual servoing tasks for either PBVS or IBVS. The goal and initial images are seen in Figure 9. In the result figures, trajectories with a black "shadow" are performed by PBVS.

Results using PBVS are seen in Figure 10. The features follow very circular trajectories, but the physical system clearly suffers from minor estimation errors. There is negligible translation motion, and the feature points quickly leave the image.

In contrast, IBVS begins with large camera retreat, pulling the feature points in towards the center of the image, as seen in Figure 11. The camera retreats over a meter before the robot encounters its joint limits. During this time the image becomes severely out of focus, but the symmetric shape of the feature points allowed the system to still calculate their position well.

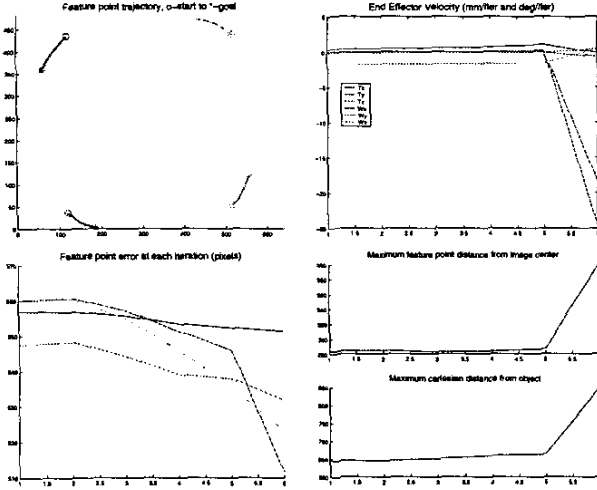


Fig. 10. PBVS Experimental Results

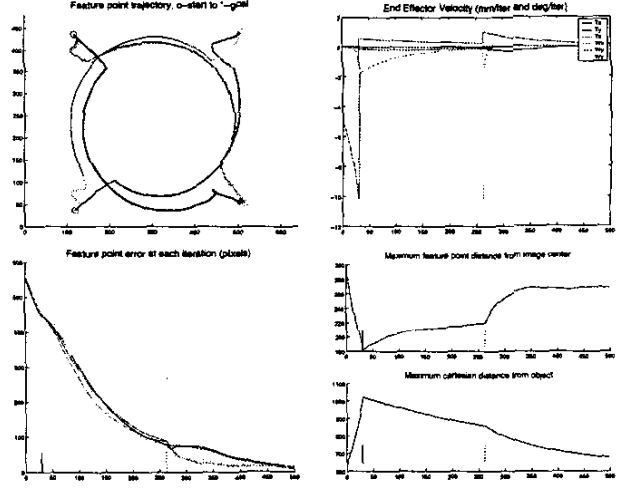


Fig. 12. Switched System Experimental Results

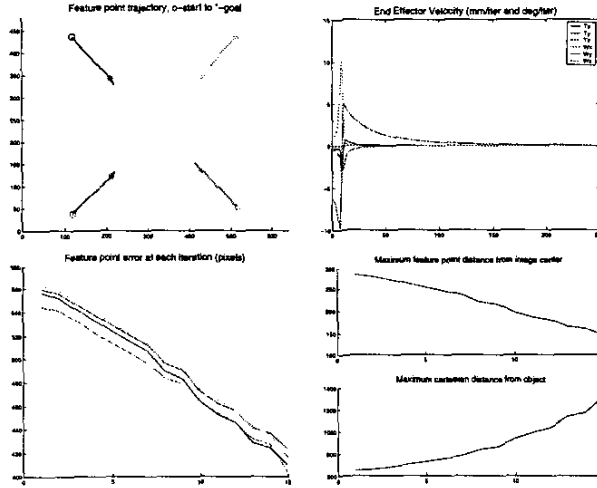


Fig. 11. IBVS Experimental Results

For the switched system we set thresholds of  $\epsilon_p = 220$  pixels and  $\epsilon_i = 1$  meter. The first threshold is slightly less than the height of the image minus the width of a feature dot. The second threshold is approximately 75. The switched system begins with IBVS and camera pull back moves the feature points towards the center of the image. However, when it hits the retreat threshold of one meter it switches to PBVS and completes the majority of the motion with well behaved rotation and undoing the effects of camera pull back. Eventually the feature points again approach the edge of the image and the system switched again to IBVS. However at this point we are in the region where either system will successfully complete visual servoing and IBVS completes the motion.

## APPENDIX

### I. PROOFS OF LEMMAS

**Lemma 1:** *The pose error  $e_p = 0$  if and only if the image error  $e_i = 0$*

PROOF. Given Assumption 1  
TO PROVE IF:

$$\begin{aligned} X_j &= R X_j^* + T \Rightarrow Z_j x_j = Z_j^* R x_j^* + T \forall j \in [1..m] \\ \text{then } e_p = 0 &\Rightarrow X_j - X_j^* = 0 \Rightarrow X_j = X_j^* \forall j \in [1..m] \\ &\Leftrightarrow R = I_3 \text{ and } T = 0 \\ &\Rightarrow Z_j = Z_j^* \text{ and } x_j = x_j \end{aligned}$$

TO PROVE ONLY IF:

$x_j = x_j^*$  implies one of four possibilities:

- 1)  $R = I_3$  and  $T = 0$
- 2)  $T$  is directed along the ray connecting the focal point to point  $p_j$
- 3)  $R \equiv u\theta$  has  $u$  oriented along the ray connecting focal point to point  $p_j$
- 4) both 2) and 3) are true

However, if we are given two or more points that do not lie on the same ray, it cannot be true that the motion is directed along the rays to both points. Since we are assumed to have at least three points for visual servoing, it must be the case that option 1) is true and the pose error  $e_p = 0$

**Lemma 2a:** *During PBVS the pose error  $e_p$  decreases monotonically while the image error  $e_i = 0$  may increase or decrease*

**Lemma 2a:** *During IBVS the image error  $e_i$  decreases monotonically while the pose error  $e_p = 0$  may increase or decrease*

PROOF. PBVS is a globally asymptotically stable (GAS), linear time varying (LTV) system with respect to the pose error, the error must decrease exponentially to zero. The image error is uncontrolled and so can increase during visual servoing. IBVS is also LTV, but is only Locally asymptotically stable (LAS) due to the possibilities of singularities in the image Jacobian (though these singularities are uncommon or impossible in a well posed physical system). The pose error is uncontrolled and can increase during visual servoing.

**Lemma 3:** For both IBVS and PBVS, there exists a range of camera positions where under visual servo control both the pose error  $e_p$  and image error  $e_i$  decrease to 0 as time goes to infinity. Additionally, one can show that if the difference between the goal and current pose consists of translation with a sufficiently small rotation, then we are within this region.

PROOF. The first statement proceeds directly from Lemmas 1 and 2.

For the second statement, the image error for each feature point,  $e_i$ , is related to the pose error during a pure translation by the equation:

$$\begin{aligned} e_i &= L_i e_p \text{ with } e_p = [T_x \ T_y \ T_z \ 0 \ 0 \ 0]^T, \ e_i = [x, y] \\ &= \begin{bmatrix} \frac{1}{z} & 0 & -\frac{x}{z} & -xy & 1+x^2 & -y \\ 0 & \frac{1}{z} & -\frac{y}{z} & -1-y^2 & xy & x \end{bmatrix} e_p \\ &= \begin{bmatrix} \frac{1}{z} & 0 & -\frac{x}{z} & -xy & 1+x^2 & -y \\ 0 & \frac{1}{z} & -\frac{y}{z} & -1-y^2 & xy & x \end{bmatrix} \begin{bmatrix} T_x \\ T_y \\ T_z \\ 0 \\ 0 \\ 0 \end{bmatrix} \\ &= -\frac{\lambda_p}{z} \begin{bmatrix} 1 & 0 & -x \\ 0 & 1 & -y \end{bmatrix} \begin{bmatrix} T_x \\ T_y \\ T_z \end{bmatrix} \end{aligned}$$

Thus, if the pose error consists of a pure translation, the image error will be an identical vector for each point, and the image error for each point will lie on a straight line. By the inverse function theorem if the error for each point is an identical vector then the pose error is a pure translation. If PBVS zeros the error, the pose trajectory will follow a straight line to the goal pose and the image errors will also remain on straight lines to their goal positions. Likewise IBVS will zero the image error along a straight line by moving the camera and reducing the pose error on a straight line. Thus for pure translations both PBVS and IBVS monotonically decrease both the image and the pose error.

Furthermore, by the Initial Condition Theorem, perturbing the translation with a sufficiently small rotation will still result in a stable system and a decrease in both image error

and pose error. We can state that the class of rotation with a translation and some sufficiently small amount of rotation can be zeroed monotonically with respect to both image and pose error by either IBVS or PBVS.

**Lemma 4:** During IBVS, the rotation component of the position error will be strictly non-increasing.

PROOF. As illustrated in [15], if a point would naturally follow a curved path in the image plane due to a camera rotation, to constrain that point to a line requires a translation backwards along the optical axis ( $T_z$ ). Furthermore the maximum distance the camera will retreat is given by

$$\frac{d_{\text{targ}}}{d_{\text{max}}} = \cos \frac{\alpha}{s}$$

where alpha is the angle in the image plane between lines from the point's goal position and current position to the image center. Thus the erroneous motions that evolve from constraining a feature point trajectory to a line involve only translations along the optical axis, never rotations of any sort. Thus the error in orientation must be decreasing or remaining steady.

#### REFERENCES

- [1] L. E. Weiss, A. C. Sanderson, and C. P. Neuman, "Dynamic sensor-based control of robots with visual feedback," *IEEE Journal of Robotics and Automation*, vol. RA-3, pp. 404-417, Oct. 1987.
- [2] J. Feddema and O. Mitchell, "Vision-guided servoing with feature-based trajectory generation," *IEEE Transactions on Robotics and Automation*, vol. 5, pp. 691-700, Oct. 1989.
- [3] P. Martinet, J. Gallice, and D. Khadraoui, "Vision based control law using 3d visual features," 1996.
- [4] S. Hutchinson, G. Hager, and P. Corke, "A tutorial on visual servo control," *IEEE Transactions on Robotics and Automation*, vol. 12, pp. 651-670, Oct. 1996.
- [5] F. Chaumette, "Potential problems of stability and convergence in image-based and position-based visual servoing," in *The confluence of vision and control* (D. Kriegman, G. Hager, and S. Morse, eds.), vol. 237 of *Lecture Notes in Control and Information Sciences*, pp. 66-78, Springer-Verlag, 1998.
- [6] N. Gans and S. Hutchinson, "An experimental study of hybrid switched system approaches to visual servoing," in *Proc. of the International Conference on Robotics and Automation, 2003*, May 2003.
- [7] M. Branicky, V. Borkar, and S. Mitter, "A unified framework for hybrid control," in *Proc. of the 33rd IEEE Conf. on Decision and Control*, 1994.
- [8] R. W. Brockett, *Hybrid models for motion control systems*. 1993. H. L. Trentelman and J. C. Willems, Eds.
- [9] D. Liberzon and A. Morse, "Basic problems in stability and design of switched systems," 1999.
- [10] M. Branicky, "Multiple Lyapunov functions and other analysis tools for switched and hybrid systems," *IEEE Trans. Automat. Contr.*, vol. 43.
- [11] V. Blondel and J. N. Tsitsiklis, "NP-hardness of some linear control design problems," *SIAM Journal on Control and Optimization*, vol. 35, no. 6, pp. 2118-2127, 1997.
- [12] O. Faugeras and F. Lustman, "Motion and structure from motion in a piecewise planar environment," 1988.
- [13] Z. Zhang and A. Hanson, "reconstruction based on homography mapping," 1996. Zhang Z. and Hanson A.R. 3d reconstruction based on homography mapping. In ARPA Image Understanding Workshop, Palm Springs, CA, 1996.
- [14] D. DeMenthon and L. S. Davis, "Model-based object pose in 25 lines of code," in *European Conference on Computer Vision*, pp. 335-343, 1992.
- [15] P. Corke and S. Hutchinson, "A new partitioned approach to image-based visual servo control," *IEEE Trans. on Robotics and Automation*, vol. 17, no. 4, pp. 507-515, 2001.